Available online at www.sciencedirect.com
SCIENCE DIRECT®
Journal of Organometallic Chemistry 680 (2003) 271–280
Journal of Organometallic Chemistry
www.elsevier.com/locate/jorganchem

1,3,2-Diazastanna-[3]ferrocenophanes bearing alkyn-1-yl groups at tin and their 1,1-organoboration with triethylborane—molecular structure of a novel spirotin compound

Bernd Wrackmeyer *, Heidi E. Maisel, Wolfgang Milius, Max Herberhold

Laboratorium für Anorganische Chemie, Universität Bayreuth, Universitaetsstr. 30, NW 1, D-95440 Bayreuth, Germany

Received 28 February 2003; received in revised form 17 April 2003; accepted 17 April 2003

Dedicated to Professor M.F. Hawthorne on the occasion of his 75th birthday

Abstract

2,2-Dichloro-1,3-bis(trimethylsilyl)-1,3,2-diazastanna-[3]ferrocenophane (**3**) reacts with lithium alkynides $LiC{\equiv}CR^1$ to give the corresponding di(alkyn-1-yl)tin derivatives **4a** ($R^1 = {}^t$Bu) and **4b** ($R^1 = SiMe_3$). 1,1-Organoboration of **4** with triethylborane affords the spirotin compounds **5** which contain both a ferrocenophane and a stannacyclopentadiene ring. The crystal structure of **5b** was determined by X-ray analysis. The compounds **4** and **5** were characterised in solution by multinuclear magnetic resonance (^{1}H-, ^{11}B-, ^{13}C-, ^{15}N-, ^{29}Si-, ^{119}Sn-NMR), using pulsed field gradients in HMBC experiments for the ^{1}H detected ^{15}N- and ^{119}Sn-NMR signals. The compound **5b** was also studied by solid-state ^{13}C, ^{29}Si and ^{119}Sn MAS NMR in order to correlate liquid and solid-state NMR data with the structural evidence.

Keywords: Ferrocene; Alkynes; Tin; Boron; Organoboration; NMR-multinuclear; X-ray

1. Introduction

The 1,1-organoboration of alkyn-1-yl metal compounds [1] has opened routes to numerous organometallic compounds, cyclic and non-cyclic, which are difficult to prepare by other methods. Among these compounds, the stanna-2,4-cyclopentadienes (stannoles) are noteworthy, since the chemistry of these reactive dienes [2] has not been systematically explored so far. We have shown that 1,1-organoboration of di(alkyn-1-yl)tin compounds proceeds smoothly to give stannoles, even in the presence of bulky substituents at the tin atom. Thus, di(alkyn-1-yl)bis(silylamino)tin derivatives **1** react with triethylborane to give stannoles **2** (Scheme 1), except when there is a *tert*-butyl group attached to the C≡C bond [3].

Recently the *N*-silylated 1,1′-diamidoferrocene has been proposed as a versatile chelating ligand by us [4] and others [5], and the convenient access to the corresponding 1,3,2-diazastanna-[3]ferrocenophane (**3**) bearing chloro substituents at the tin atom [4] permits the synthesis of the di(alkyn-1-yl)tin compounds **4**. These can then be used in 1,1-organoboration reactions. In the present work, we report on the compounds **4**, and on their conversion into stannoles **5**. The latter are novel spirotin compounds, and hence X-ray structural analysis was performed for one of them. Extensive NMR studies in solution and in the solid state were also carried out.

* Corresponding author. Tel.: +49-921-552542; fax: +49-921-552157.
E-mail address: b.wrack@uni-bayreuth.de (B. Wrackmeyer).

0022-328X/03/$ - see front matter © 2003 Elsevier Science B.V. All rights reserved.
doi:10.1016/S0022-328X(03)00401-7

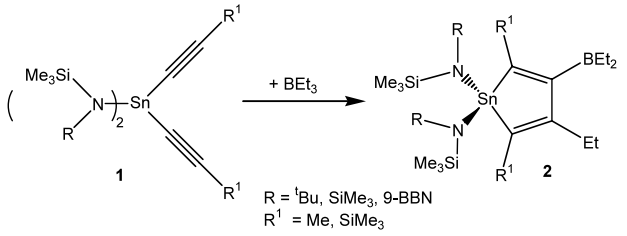

Scheme 1.

alkene with a stereochemistry at the C=C bond precluding ring closure. Since 1,1-organoboration is reversible [1], the reaction can finally be driven to provide **5b**. Although intermediates other than **6b** were not observed in the present work, it can be assumed that zwitterionic intermediates of the type **7** are formed prior to the ring closure to the stannoles **5**. Such intermediates have been detected, isolated and structurally characterised in similar 1,1-organoboration reactions [1,6].

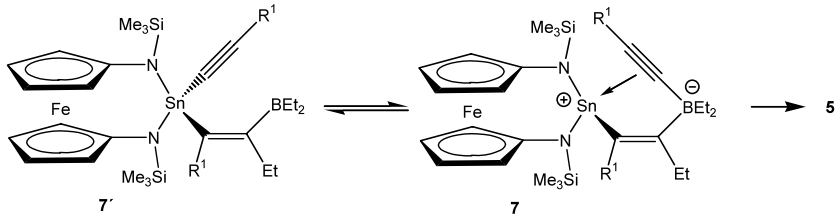

2. Results and discussion

2.1. Synthesis of the 2,2-di(alkyn-1-yl)-1,3,2-diazastanna-[3]ferrocenophanes (4) and their reactivity towards triethylborane

The results of the preparative work are summarized in Scheme 2. The [3]ferrocenophane **3** reacts with lithium alkynides to give the di(alkyn-1-yl)tin derivatives **4** in high yield and high purity. The compounds **4** are yellow solids, sensitive to air and moisture, readily soluble in benzene or toluene, and they can be stored in the refrigerator for prolonged periods.

When solutions of **4** in toluene are treated with an excess of triethylborane at room temperature, a slow reaction starts in the case of **4b**, whereas **4a** does not react. However, heating of the reaction mixture at 80 °C for several hours leads to complete conversion of **4b** into the spirotin compound **5b**. In the case of **4a**, the mixture with triethylborane was kept at 90 °C for six days in order to promote conversion (> 80%) to **5a**. In the compounds **5** both the 1,3,2-diazastanna-[3]ferrocenophane and the stannacyclopentadiene moieties are present. In contrast to the reaction shown in Scheme 1, where the compounds **1** with $R^1 = SiMe_3$ do not react with BEt_3 at room temperature, and 1,1-organoboration does not take place at all when $R^1 = {}^t$Bu, even under rather harsh reaction conditions, the conversion of **4** to **5** proceeds smoothly. The slow reaction of **4b** with Et_3B at room temperature permits identification of an intermediate **6b** by monitoring the progress of the reaction with ^{29}Si-NMR spectroscopy (vide infra). In **6b**, the 1,1-organoboration of the first Sn–C≡ bond has led to an

The compounds **5a** and **5b** were isolated as yellow, air- and moisture-sensitive solids, and recrystallisation of **5b** from pentane at −20 °C gave single crystals suitable for X-ray crystallography (vide infra). Compound **5a** always contained a small amount of the starting material **4a** along with some unidentified decomposition products, as a result of the reaction conditions, and could not be completely purified. Both **5a** and **5b** are readily soluble in benzene; diluted solutions can be kept for several months in the refrigerator, and the solid material can be stored in the same way.

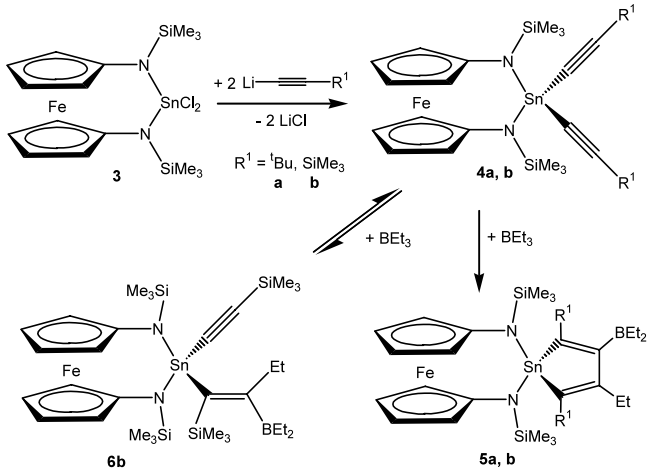

Scheme 2.

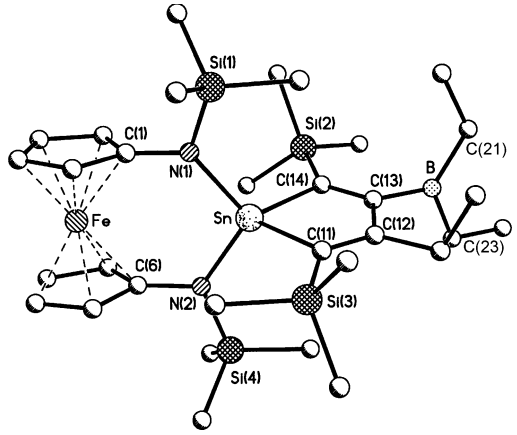

Fig. 1. Molecular structure of the spiro compound **5b** (hydrogen atoms are omitted for clarity); selected bond lengths (pm) and angles (°): Sn–N(1) 204.6(4), Sn–N(2) 204.2(4), Sn–C(11) 214.8(5), Sn–C(14) 216.7(5), Si(1)–N(1) 173.8(4), Si(4)–N(2) 174.4(4), N(1)–C(1) 142.1(7), N(2)–C(6) 143.6(7), Si(2)–C(14) 185.8(6), Si(3)–C(11) 185.9(6), C(11)–C(12) 133.0(7), C(12)–C(13) 155.8(8), C(13)–C(14) 133.7(7), B–C(13) 157.5(9), B–C(21) 154.8(9), B–C(23) 157.3(9), C(12)–C(25) 150.4(8), Fe-ring centroid 163.3 and 163.7, Fe–Sn 384.5; N(1)–Sn–N(2) 109.03(17), C(11)–Sn–C(14) 85.5(2), C(1)–N(1)–Sn 122.5(3), Si(1)–N(1)–Sn 124.1, Si(4)–N(2)–Sn 126.0(2), C(12)–C(11)–Si(3) 130.6(4), C(12)–C(11)–Sn 106.2(4), Si(2)–C(14)–Sn 119.9(3), Si(3)–C(11)–Sn 123.0(3), C(11)–C(12)–C(13) 121,7(5), C(21)–B–C(13) 123.3(6), C(23)–B–C(13) 117.2(5), C(21)–B–C(23) 119.6(6), C(22)–C(21)–B 120.5(6), C(24)–C(23)–B 120.4(6).

2.2. Crystal structure of the spirotin compound *5b*

The molecular structure of **5b** is shown in Fig. 1 together with selected bond lengths and angles. The ferrocene geometry is clearly distorted, in contrast to the situation in **3** [4]. The planes of the cyclopentadienyl rings in **5b** deviate from the eclipsed position by $\tau = 9.2°$, and are tilted towards the tin atom with an angle $\alpha = 3.0°$. Thus, the arrangement of the atoms Fe, C(1), N(1), Sn is non-planar, whereas the stannole ring is almost planar (mean deviation 1.2 pm). The Sn–N distances in **5b** (204.3(4) and 204.6(4) pm) are longer than in **3** (199.5(2) pm), and the bond angle N–Sn–N in **5b** (109.03(17)°) is more acute than in **3** (117.1(1)°). The N–Sn–N plane and the stannole ring in **5b** form an angle of 86.2°. Other molecular structures to compare with **5b** are those of the stannole **2** (R = 9-BBN; R^1 = $SiMe_3$) [3], the spiro-bistannole **8** [7] and the spirostannole **9** [7].

Table 1
^{13}C-, ^{15}N-, ^{29}Si- and ^{119}Sn-NMR data [a] of the di(alkyn-1-yl)tin compounds **4a** and **4b**, and of **1** (R = R^1 = $SiMe_3$) [2] for comparison

Compound R^1	**4a** ^{t}Bu	**4b** $SiMe_3$	**1** $SiMe_3$; R = $SiMe_3$
$\delta^{13}C(Sn–C\equiv)$	105.3 [1014.0]	113.3 [873.0] (10.6)	115.2 [912.8] (10.4)
$\delta^{13}C(R^1–C\equiv)$	119.8 [193.8]	119.5 [137.9] (73.7)	119.1 [148.1] (73.9)
$\delta^{13}C(R^1)$	28.5 [14.8] (C) 30.5 [7.4](Me)	−0.6 [< 3] (56.1)	−0.6 (56.0)
$\delta^{13}C(N–SiMe_3)$	2.6 [< 2] (56.1)	2.5 [6.6] (56.5)	5.6 [14.2} (55.8)
$\delta^{13}C(fc\text{-}C^1)$	105.3 [29.6]	105.0 [31.9]	–
$\delta^{13}C(fc\text{-}C^{2,5})$	68.6 [14.8]	68.8[15.6]	–
$\delta^{13}C(fc\text{-}C^{3,4})$	65.8 [< 3]	66.1 [3.0]	–
$\delta^{15}N$	n.m.	−351.7 [124.4] (10.2)	−343.1 [62.2] (6.1)
$\delta^{29}Si$	11.5 [61.0] N–Si	12.3 [61.0] N–Si	7.6 [9.0] N–Si
	–	−17.9 [15.4] ≡C–Si	−18.2 [16.5] ≡C–Si
$\delta^{119}Sn$	−221.9	−247.5	−248.2

[a] Measured in C_6D_6 at 23 ± 1 °C.; coupling constants $J(^{119}Sn,X)$ [± 0.5 Hz] are given in brackets, $J(^{29}Si,X)$ [±0.1 Hz] in parentheses; n.m. means not measured.

The structural data for **5b** show some agreement with **2** as far as the bond lengths and bond angles at the tin atoms are concerned (**5b**: N(1)–Sn–N(2) 109.03(17)°, C(11)–Sn–C(14) 85.5(2)°; **2**: N–Sn–N 108.94(8)°, C–Sn–C 86.1(1)°). In the cases of **8** and **9**, all endocyclic bond angles C–Sn–C are small. Large differences become obvious by comparing the corresponding bond angles at the carbon atoms next to tin in **5b** (Si(2)–C(14)–Sn 119.9(3)°, Si(3)–C(11)–Sn 123.0(3)°), in **2** with R = 9-BBN and R^1 = $SiMe_3$ (128.47(15) and 136.68(14)°), and in **8** (123.1 and 120.3°). Apparently, the trimethylsilyl groups at the carbon atoms in **5b** and **8** are less affected by steric repulsion than in **2**. The C(12)–C(13) bond in the stannole ring in **5b**, and its equivalent in **2** and **8** are rather long, at 155.8(8), 152.8(4) and 153.0(6) pm, respectively, possibly as a result of hyperconjugation due to the orientation of the boryl group. In **5b** the angle between the plane of the stannole ring and the plane defined by C(21),B and C(23), a measure of the relationship of the planes in terms of twist about the C(13)–B bond joining them,

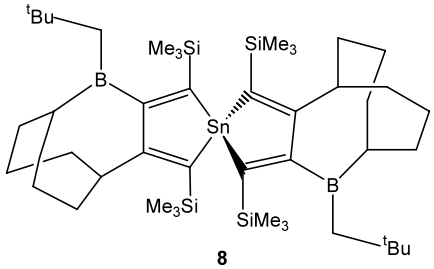

8

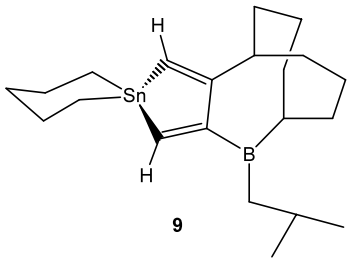

9

Table 2
^{119}Sn-, ^{29}Si-, ^{15}N-, ^{13}C-, and ^{11}B-NMR data [a] of the stannoles **5a** and **5b**; data for **2** (R = R^1 = SiMe$_3$) [2], the spirobistannole **8** [b] (R^1 = SiMe$_3$) [7] and the dimethyltin derivative **10** [8] are given for comparison

	5a (R^1 = ^{t}Bu)	**5b** (R^1 = SiMe$_3$)	**2** (R = R^1 = SiMe$_3$)	**8** (R^1 = SiMe$_3$)	**10** (R^1 = SiMe$_3$)
δ^{13}C(2)	153.7 [500.0]	143.7 [210.2] (64.4)	146.4 [284.5]	144.1 [121.0] (64.4)	145.0 [194.2] (65.0)
δ^{13}C(3)	156.5 (br) [30.0]	175.9 (br) [25.0]	175.9 (br)	182.3 (br)	181.8 (br)
δ^{13}C(4)	147.8 [217.0]	162.5 [108.0]	163.1 [182.1]	168.3 [85.9]	166.7 [94.8]
δ^{13}C(5)	146.3 [542.0]	133.9 [292.0] (64.4)	139.3 [373.6]	138.1 [183.7] (63.3)	139.1 [260.4] (63.6)
δ^{13}C(2,5-R^1)	37.9 [76.0] (C)	2.3 [9.5] (52.0)	3.9 [12.6] (51.8)	2.2 [10.7] (52.0)	1.9 [9.0] (51.9)
	33.6 [25.0] (Me)	2.3 [9.5] (52.0)	4.0 [11.0] (52.3)	2.2 [11.4] (51.4)	1.7 [11.7] (51.9)
	36.7 [69.5] (C)				
	33.8 [23.0] (Me)				
δ^{13}C(BEt$_2$)	23.2 (br), 10.6	23.1 (br), 9.9	23.2 (br), 9.8	23.0 (br), 9.7	22.3 (br), 9.3
δ^{13}C(4-Et)	28.0 [112.3]	32.7 [127.8]	32.5 [134.8]	32.1 [87.0]	31.4 [92.2]
	14.6 [n.m.]	14.6 [10.2]	15.6 [13.0]	15.7	16.0 [9.7]
δ^{13}C(NSiMe$_3$)	2.0 [< 2] (56.1)	1.8 [< 5] (56.1)	7.1 [9.4] (55.3)	–	–
δ^{13}C(fc-C^1)	106.6 [28.0]	106.8 [24.0]	–	–	–
δ^{13}C(fc-C^{2,5})	69.1 [5.0]	69.9 [4.8]	–	–	–
		69.2 [4.7]			
δ^{13}C(fc-C^{3,4})	65.9 [< 2]	66.2 [< 2]	–	–	–
	64.5 [< 2]				
δ^{119}Sn	37.0	107.5 [c]	10.2	222.1	133.5
δ^{29}Si(NSi)	7.6 [76.1]	8.4 [74.0] [d]	4.4 [5.7]	−7.3 [98.1]	−8.2 [98.2]
δ^{29}Si(2,5-Si)	–	−7.3 [115.0] [e]	−6.3 [132.5]	−8.9 [96.1]	−9.7 [97.4]
		−8.4 [111.6] [e]	−8.0 [140.2]		
δ^{15}N	−351.8 [64.5]	−349.4 [91.0]	−337.7 [135.2] (5.3)	–	δ^{13}C(SnMe$_2$): −5.6 [259.1]
δ^{11}B	88.5 ± 1	89.5 ± 1	87 ± 1	86 ± 1	85 ± 1

[a] In C_6D_6 at 23 °C. All coupling constants to ^{119}Sn [±0.5 Hz] are given in brackets, and to ^{29}Si (±0.1 Hz) in parentheses; (br) denotes broad signals due to partially relaxed ^{13}C–$^{10/11}$B coupling; n.m. means not measured. The numbering has been selected for best comparison with other compounds, and is not in agreement with nomenclature.
[b] Prepared from Sn(C≡C–SiMe$_3$)$_4$ and BEt$_3$.
[c] Solid state: 104.3 (see Fig. 6).
[d] Solid state: 8.8, 8.2.
[e] Solid state: −6.4, −7.5.

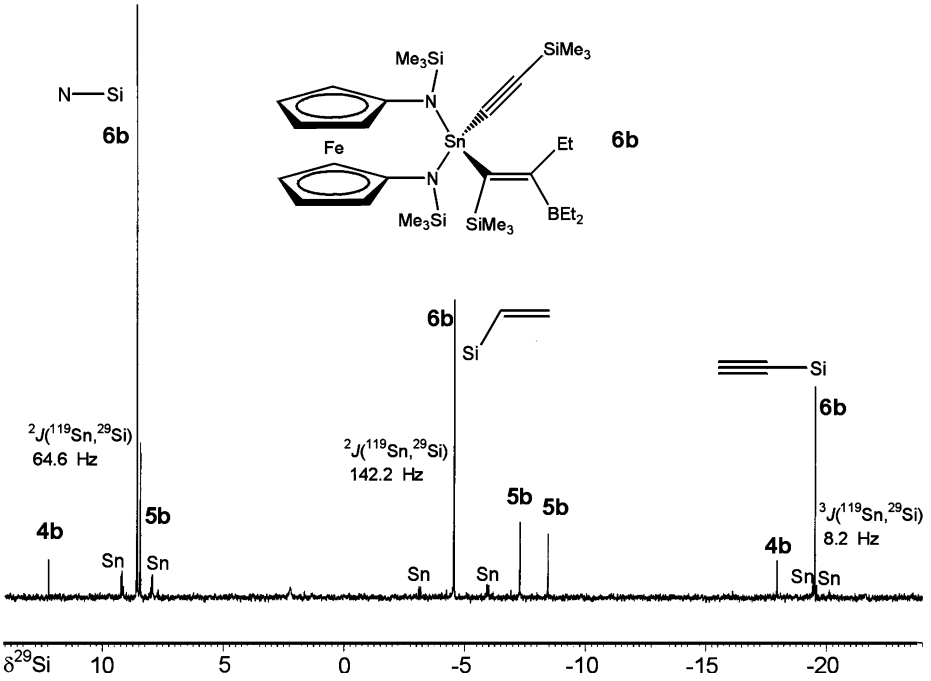

Fig. 2. 49.9 MHz ^{29}Si{^{1}H}-NMR spectrum of the reaction solution containing **4b** and an excess of BEt$_3$, recorded by using the refocused INEPT pulse sequence [12]. In addition to the ^{29}Si-NMR signals of the intermediate **6b**, the ^{29}Si-NMR signals of the starting material **4b** are still visible as well as those of the final product **5b**.

Table 3
NMR data [a,b] of the intermediate **6b**, observed in the course of the reaction of **4b** with triethylborane

Compound	**6b** $R^1 = SiMe_3$
$\delta^{13}C(Sn-C\equiv)$	116.9
$\delta^{13}C(R^1-C\equiv)$	123.3
$\delta^{13}C(R^1)$	−0.2 (≡C–Si*Me*$_3$), 2.9 (=C–Si*Me*$_3$)
$\delta^{13}C(N-SiMe_3)$	2.7
$\delta^{13}C(fc\text{-}C^1)$	106.9 [35.8]
$\delta^{13}C(fc\text{-}C^{2,5})$	69.3, 68.4
$\delta^{13}C(fc\text{-}C^{3,4})$	66.3, 65.4
$\delta^{13}C(Sn-C=)$	142.6
$\delta^{13}C(B-C=)$	186.0 (br)
$\delta^{13}C(=C-Et)$	38.5 [165.0], 13.2 [13.0]
$\delta^{13}C(BEt_2)$	22.3 (br), 9.7
$\delta^{29}Si$	8.5 [64.6] (N–Si), −4.5 [142.4] (=C–Si), −19.5 [8.2] (≡C–Si)
$\delta^{119}Sn$	−175.5

[a] In C_6D_6 at 23 °C. All coupling constants to ^{119}Sn [±0.5 Hz] are given in brackets; (br) denotes broad signals due to partially relaxed $^{13}C-^{10/11}B$ coupling.
[b] ^1H-NMR: $\delta^1H^{3,4} = 3.83$ (m), 3.84 (m), $\delta^1H^{2,5} = 4.11$ (m), 4.31 (m); δ^1H (=C–CH_2) = 2.87 (q); all other signals overlap with those of BEt_3, **4b**, and **5b**.

and the corresponding angle in **2** and **8** are 77, 86.4, 60 and 63.2°, respectively. In contrast, in **9** the same C–C bond is shorter (150.6(3) pm) and the interplanar angle is only 47.3°. Also the angles at C(21) and C(23), the ethyl carbon atoms directly atttached to boron, in **5b** are much greater (120.5(6) and 120.4(6)°) than the tetrahedral angle, possibly also as a consequence of hyperconjugation [9].

2.3. NMR spectroscopic results

The solution-state NMR data of the compounds **4** (Table 1) and **5** (Table 2) strongly support the proposed structures. The intermediate **6b** was first identified by its ^{29}Si-NMR spectrum (see Fig. 2), and subsequently a consistent set of ^1H-, ^{13}C-, and ^{119}Sn-NMR data was also collected (Table 3). All nuclei (^1H, ^{11}B, ^{13}C, ^{15}N, ^{29}Si, ^{119}Sn) provide important and complementary information on the structures. Solution-state ^1H, ^{11}B and in most cases ^{13}C-NMR spectra can be measured by routine NMR techniques, whereas the measurement of useful ^{15}N-, ^{29}Si- and also ^{119}Sn-NMR spectra, for the problems encountered here, required a more sophisticated approach (vide infra). The ^{11}B-NMR signals are found at high frequencies as very broad ($h_{1/2} > 700$ Hz) singlets in the typical region of trigonal organoboranes without BC(pp)π interactions [10]. Since these signals can only be observed properly in the absence of triethylborane, ^{11}B-NMR is not helpful for monitoring the reactions.

In the case of **5b**, where the crystal structure is known, solid-state ^{13}C, ^{29}Si and ^{119}Sn MAS NMR spectra were measured. These showed all the expected features in conformity with the crystal structure, and the isotropic chemical shifts are in good agreement with the data for solutions of **5b** (see Fig. 3 for the comparison of solution and solid-state ^{13}C MAS NMR spectra of **5b** in the range of the olefinic carbon atoms). In the solid state, in contrast to solutions, two different ^{13}C-NMR signals are observed for the quaternary ferrocene carbon atoms, and also two different ^{29}Si-NMR signals for the $NSiMe_3$ groups, since these atoms or groups are crystallographically non-equivalent [see Fig. 1: C(1), C(6), and Si(1), Si(4)].

In solution, the ferrocene $C^{2,5}$ and $C^{3,4}$ atoms should show two signals both due to the unsymmetric substitution of the stannole ring. This is observed for $C^{3,4}$ in the case of **5a** (the different $^{13}C^2$ and $^{13}C^5$ resonances were not resolved), and for $C^{2,5}$ in the case of **5b** (here the difference between the $^{13}C^3$ and $^{13}C^4$ resonances was too small). The assignment of these ^{13}C-NMR signals was based on 1D $^1H/^1H$ NOE difference experiments [11], where selective irradiation in the $^1H(SiMe_3)$ resonance gave a response only for the ^1H nuclei in 2,5-position of the ferrocene unit, followed by $^{13}C/^1H$ HETCOR experiments. Apparently, the effect is too small for observation of non-equivalence of H^2, H^5 and H^3, H^4 (^1H-NMR spectra were measured at 500 MHz). In **6b**, the greater difference in the nature of the subtsituents at the tin atom is reflected by the resolution of four separate ^{13}C and ^1H resonance signals for the $C^{2,3,4,5}$ and $H^{2,3,4,5}$ atoms (Table 3).

Apart from the chemical shift $\delta^{15}N$, the coupling constant $^1J(^{117/119}Sn,^{15}N)$, to be determined from the $^{117/119}Sn$ satellites in the ^{15}N-NMR spectra, is of particular interest. It was not possible to measure ^{15}N-NMR spectra at natural abundance of the compounds **4** or **5** directly, and the measurements were still rather time-consuming (6–12 h) using the INEPT pulse sequence [12], taking advantage of the small coupling constant $^3J(^{15}N,Si,C,^1H)$. Therefore, the application of indirect detection with the HMBC technique [13] was explored. Using the gradient-enhanced version of this pulse sequence [14], the best result was obtained by assuming $^3J(^{15}N,Si,C,^1H) = 1$ Hz, as shown in Fig. 4 for **5b**. These measurements require less than 1 h of spectrometer time, and diluted solutions should be studied in order to avoid effects due to radiation dumping [17].

A comparison of the data $^1J(^{119}Sn,^{15}N)$ for **4a**,**b** with those of other di(alkyn-1-yl)bis(amino)tin compounds [3,18] suggests a positive sign, whereas a negative sign of $^1J(^{119}Sn,^{15}N)$ is more likely in the case of **5** [3,6d]. Work is in progress to determine these signs, using experiments similar to that shown in Fig. 4, where the tilt of the cross peaks for the $^{117/119}Sn$ satellites gives information on the relative coupling signs of $^4J(^{117/119}Sn,^1H)$ and $^1J(^{117/119}Sn,^{15}N)$.

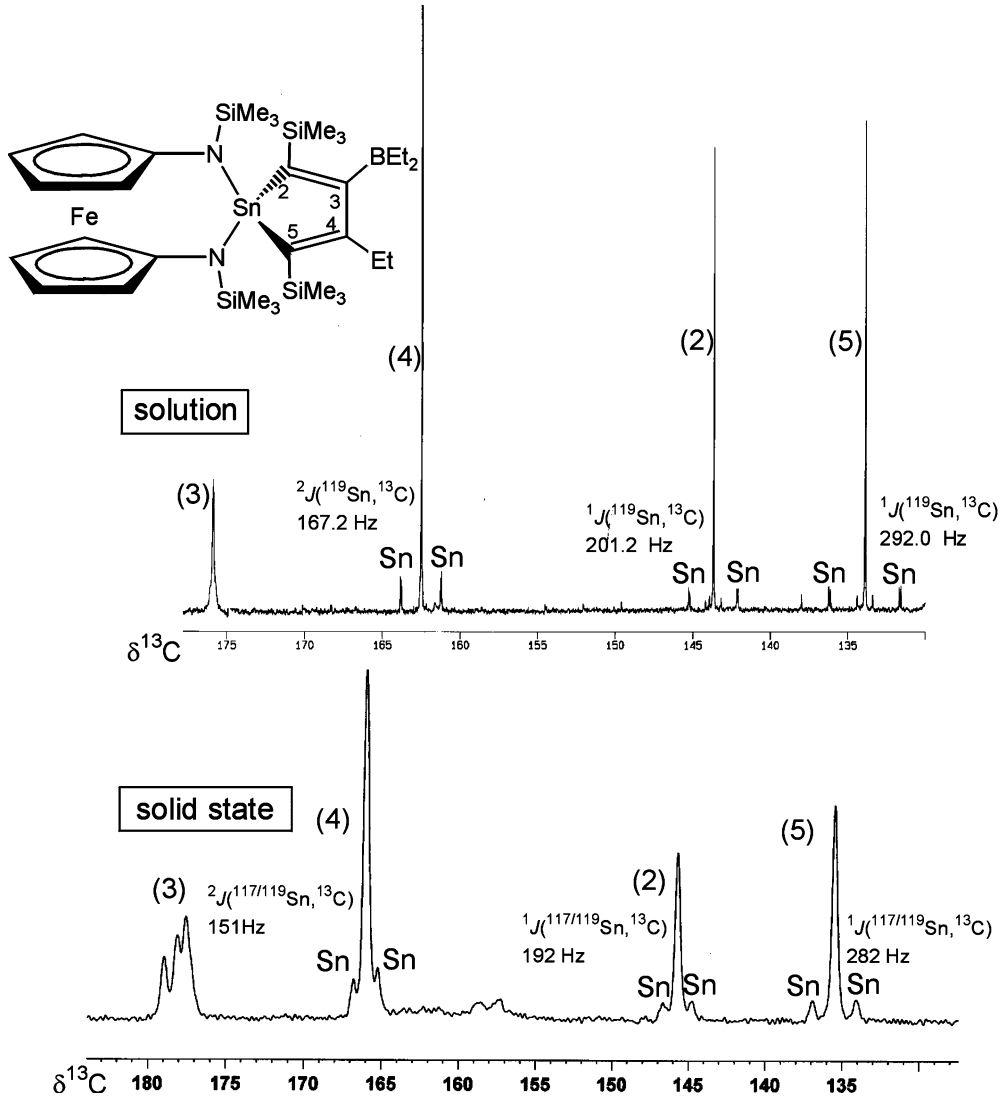

Fig. 3. $^{13}C\{^1H\}$-NMR spectra in solution (62.9 MHz) and in the solid state (MAS, 100.6 MHz; 4 mm rotor; 10 000 transients; repetition time 5 s; spinning speed 9 kHz) of **5b** showing the regions for the olefinic carbon atoms of the stannacyclopentadiene moiety. Chemical shifts $\delta^{13}C$ and coupling constants $J(Sn,^{13}C)$ are almost identical in both phases ($^{117/119}Sn$ satellites corresponding to $^1J(Sn,^{13}C)$ and $^2J(Sn,^{13}C)$ are indicated). In the solid-state MAS NMR spectrum, the satellites overlap due to the greater line width. In the liquid-state NMR spectrum, the $^{13}C(3)$ signal is typically broad [15] due to unresolved (partially relaxed) scalar $^{13}C-^{11}B$ coupling. The analogous signal in the solid-state MAS NMR spectrum is split because of non-averaged interactions of ^{13}C with the quadrupolar ^{11}B nucleus [16] combined with splitting due to scalar $^{13}C-^{11}B$ spin–spin coupling.

As shown in Fig. 2, ^{29}Si-NMR spectra, measured by INEPT [11], give satisfactory results for most purposes, including monitoring of the progress of the reactions studied here. In principle, ^{119}Sn-NMR [19] should give at least the same or complementary information. However, for diluted reaction solutions we have encountered difficulties, since the magnitude of the long-range coupling constants $^nJ(^{119}Sn,^1H)$ ($n > 3$) is too small for efficient INEPT experiments, considering that the ^{119}Sn-NMR signals are significantly broadened by unresolved scalar $^{119}Sn-^{14}N$ (in **4**), and also $^{119}Sn-^{11}B$ (in **5**) spin–spin coupling. Application of high field spectrometers is not really helpful because efficient nuclear spin relaxation of ^{119}Sn by the chemical-shift-anisotropy mechanism further increases the line widths. Again, we have explored the application of the gradient-enhanced HMBC technique assuming $^nJ(^{119}Sn,^1H) = 2$ Hz. The result for **5b** is shown in Fig. 5. Not only does it provide the information on $\delta^{119}Sn$ within very short time but it also indicates which ^1H nuclei have still a small coupling interaction with ^{119}Sn [20].

According to the crystal structure, there is only one tin site in the solid **5b**. The solid-state $^{119}Sn\{^1H\}$ MAS NMR spectrum (Fig. 6) confirms this, and, in agreement with the solid-state ^{13}C and ^{29}Si MAS NMR spectra, it rules out polymorphism of the bulk material. The spinning sideband pattern in Fig. 6 shows that the shielding tensor of ^{119}Sn is completely asymmetric, typical of organotin compounds with low local symmetry at the site of the tin atom [21], and that the chemical

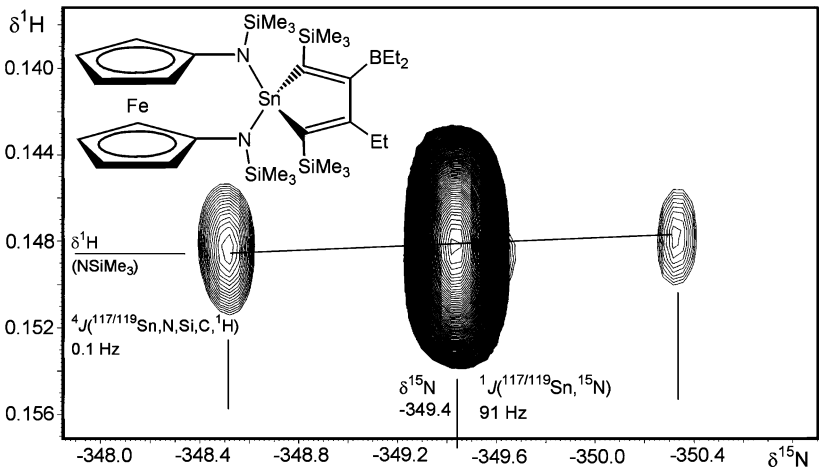

Fig. 4. Contour plot of the 500 MHz 2D $^{1}H/^{15}N$ gradient-enhanced HMBC experiment [14] of **5b** (8 mg dissolved in 0.6 ml of C_6D_6), based on a long-range coupling constant $^{3}J(^{15}N,Si,C,^{1}H)$. The spectrum is the result of 128 experiments with eight transients each with a FID resolution of 8 Hz in F_1 (^{15}N) and 0.05 Hz in F_2 (^{1}H) (40 min of spectrometer time). The small positive tilt of the cross peaks reveals $^{4}J(^{117/119}Sn,N,Si,C,^{1}H) = 0.1$ Hz, and indicates that the signs of the reduced coupling constants $^{4}K(^{117/119}Sn,^{1}H)$ and $^{1}K(^{117/119}Sn,^{15}N)$ are alike.

shift anisotropy is in the order of 800 ppm (similar to **8** [7]). The centre band (and of course also the side bands) possesses a fine structure which is the result of both non-averaged dipolar interactions of ^{119}Sn with the two quadrupolar ^{14}N nuclei [16] and scalar $^{119}Sn-^{14}N$ spin–spin coupling [$^{1}J(^{119}Sn,^{14}N)$]. The residual broadening of the ^{119}Sn-NMR signal is too large for a meaningful simulation using the known value of $^{1}J(^{119}Sn,^{14}N)$ ($0.713\ ^{1}J(^{119}Sn^{15}N) \approx 66$ Hz).

3. Conclusions

The substitution of both chloro ligands at the tin atom in **3** by alkyn-1-yl groups to give **4** is straightforward. The compounds **4** are fairly stable and survive (e.g. **4a**) heating at 90 °C in toluene solution for several days. 1,1-Organoboration of **4** with triethylborane converts the di(alkyn-1-yl)tin moiety into the stannacyclopentadiene ring in **5**, a novel type of spirotin

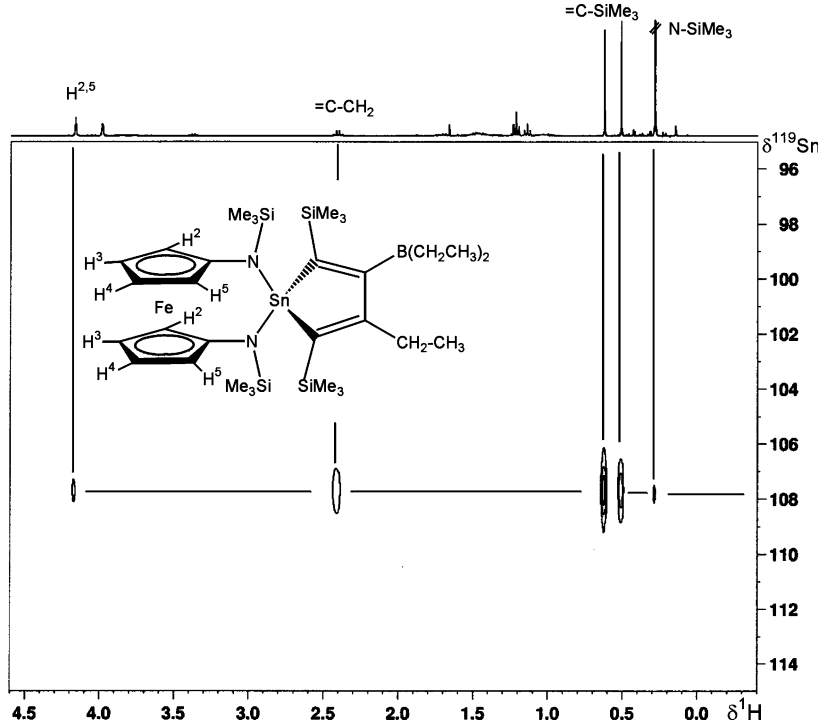

Fig. 5. Contour plot of the 400 MHz 2D $^{1}H/^{119}Sn$ gradient-enhanced HMBC experiment [14,20] of **5b** (8 mg dissolved in 0.6 ml of C_6D_6), based on a long-range coupling constant $^{n}J(^{119}Sn,^{1}H) = 2$ Hz ($n > 3$). The spectrum is the result of 64 experiments with four transients each, and required 8 min of spectrometer time. The cross peaks indicate weak coupling to all $^{1}H(SiMe_3)$, to $^{1}H(=C-CH_2)$, and $^{1}H(fc-H^{2,5})$ nuclei.

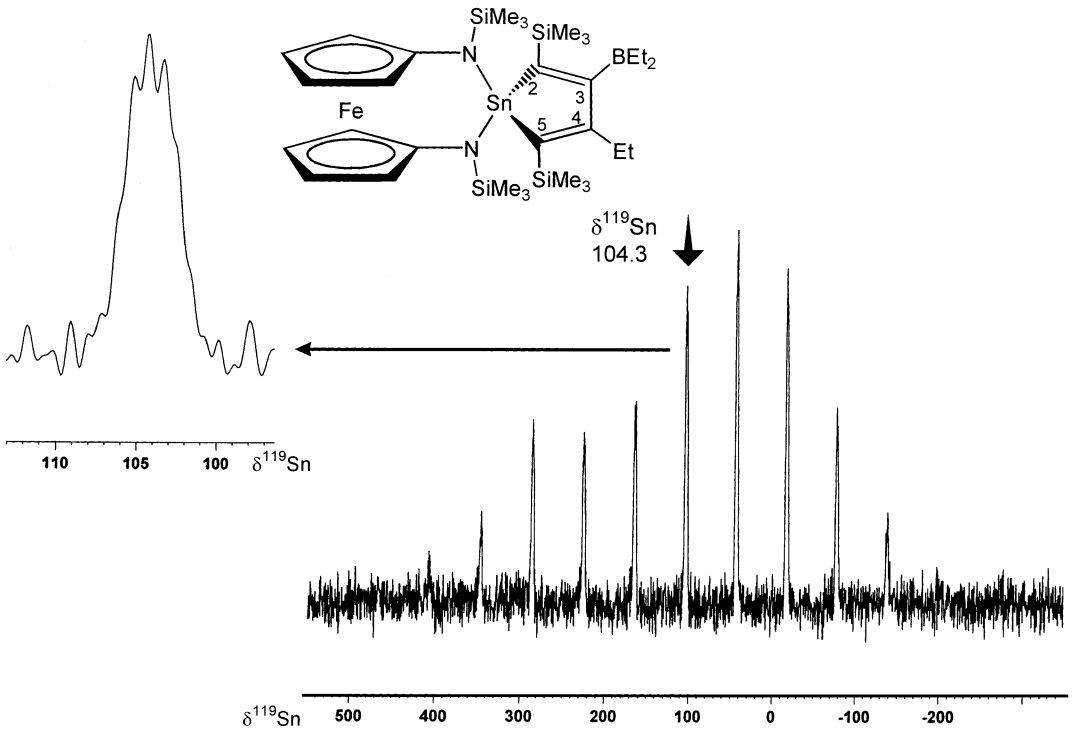

Fig. 6. 149.2 MHz solid-state $^{119}Sn\{^{1}H\}$ MAS NMR spectrum of the stannole **5b** (4 mm rotor; spinning speed 9 kHz; 516 transients, repetition time 5 s; the isotropic chemical shift $\delta^{119}Sn$, confirmed by measurments at different spinning rates, is indicated). The side band pattern shows the typically large anisotropy of the shielding tensor. The splitting (expansion of the centre band is shown) results from dipolar interactions between ^{119}Sn and the two quadrupolar ^{14}N nuclei [16] together with scalar $^{119}Sn-^{14}N$ spin–spin coupling.

compound. Apparently, the chelating ability of the 1,1′-bis(*N*-trimethylsilylamido)ferrocene unit in **3** is sufficient to allow for many reactions, typical of organotin compounds, without degradation of the 1,3,2-diaza-[3]ferrocenophane system. Clearly, the compounds **4** and **5** also provide a playground for testing NMR spectroscopic techniques.

4. Experimental

4.1. General

All compounds were prepared and handled in an atmosphere of dry argon, and carefully dried solvents and oven-dried glassware were used throughout. The starting materials such as BuLi in hexane (1.6 M), the alkynes and triethylborane were commercially available, and **3** was prepared as described [4]. NMR measurements in C_6D_6 with samples in 5 mm tubes at 23 ± 1 °C: Bruker ARX 250, Bruker Avance 400, Bruker DRX 500, Varian Inova 500 for ^{1}H-, ^{11}B-, ^{13}C-, ^{15}N-, ^{29}Si-, and ^{119}Sn-NMR; chemical shifts are given with respect to Me_4Si [$\delta^{1}H$ (C_6D_5H) = 7.15; $\delta^{13}C$ (C_6D_6) = 128.0; $\delta^{29}Si = 0$ for $\Xi(^{29}Si) = 19.867184$ MHz]; external neat nitromethane [$\delta^{15}N = 0$ for $\Xi(^{15}N) = 10.136767$ MHz], external BF_3–OEt_2 [$\delta^{11}B = 0$ for $\Xi(^{11}B) = 32.083971$ MHz], external Me_4Sn [$\delta^{119}Sn = 0$ for $\Xi(^{119}Sn) = 37.290665$ MHz]. Solid-state ^{13}C, ^{29}Si and ^{119}Sn MAS NMR spectra (with variable amplitude cross polarisation [22]) of **5b** were measured from a sample packed under argon in a 4 mm ZrO_2 rotor, using a Bruker Avance 400 NMR spectrometer equipped with a CP MAS unit, and isotropic chemical shifts are given with respect to the same reference compounds as for liquids. Melting points (uncorrected): Büchi 510 melting point apparatus.

4.2. Synthesis of the 2,2-di(alkyn-1-yl)-1,3-bis(trimethylsilyl)-1,3,2-diazastanna-[3]ferrocenophanes *4a,b*

A freshly prepared suspension of the respective lithium alkynide (1.6 mmol) in hexane (25 ml) was cooled to −30 °C, and **3** (0.44 g, 0.8 mmol) dissolved in hexane (20 ml) was added under vigorous stirring. After warming to room temperature (r.t.), the mixture was kept stirring for 2 h, and insoluble material was filtered off. Evaporation of the hexane in vacuo left a viscous light yellow oil which slowly solidified (yield > 85%), and was identified as pure (> 95% according to ^{1}H-NMR) **4a** and **4b**, respectively. **4a**: ^{1}H-NMR (C_6D_6; 250 MHz): $\delta = 0.42$ (s, 18H, N–$SiMe_3$), 1.10 (s, 18H, ≡C–^{t}Bu), 3.88 (m, 4H, $H^{3,4}$), 4.21 (m, 4H, $H^{2,5}$); **4b**:

^{1}H-NMR (C_6D_6; 250 MHz): $\delta = 0.09$ (s, 18H, ≡C–$SiMe_3$), 0.35 (s, 18H, N–$SiMe_3$), 3.80 (m, 4H, $H^{3,4}$), 4.12 (m, 4H, $H^{2,5}$).

4.3. 1,1-Organoboration of the ferrocenophanes 4—synthesis of the stannoles 5

The compounds **4a** or **4b** (0.1 mmol) were dissolved in toluene, and triethylborane (0.7 ml, 5 mmol) was added in one portion at r.t. Monitoring of the reaction progress by ^{29}Si-NMR indicated that a slow reaction started already at r.t. in the case of **4b**, whereas, under these conditions, **4a** remained unreacted. After 6 days at 90 °C most of **4a** was converted into **5a** (yield > 85%) which, however, could not be completely purified. After 2 days at r.t., most of **4b** was consumed, an intermediate **6b** was formed along with a small amount of the final product **5b** (see Fig. 2). Heating the mixture at 70 °C for 18 h afforded pure **5b** (yield > 95%). After evaporation of benzene in vacuo, the remaining yellow solid was dissolved in pentane and crystalline material (m.p. 148 °C; the colour of the crystals start to become dark above 105 °C) suitable for X-ray structural analysis and solid-state NMR spectra were obtained at −20 °C. **5a**: ^{1}H-NMR (C_6D_6; 250 MHz): $\delta = 0.23$ (s, 18H, N–$SiMe_3$), 1.22, 1.39 (s, s, 9H, 9H, =C–^{t}Bu), 2.03 (m, 2H, =C–CH_2), 1.03 (t, 3H, –CH_3), 1.25–0.90 (m, 10H, BEt_2), 3.84 (m, 4H, $H^{3,4}$), 4.38 (m, 4H, $H^{2,5}$); **5b**: ^{1}H-NMR (C_6D_6; 250 MHz): $\delta = 0.09$ (s, 18H, N–$SiMe_3$), 0.34, 0.45 (s, s, 9H, 9H, =C–$SiMe_3$), 2.26 (m, 2H, =C–CH_2), 0.93 (t, 3H, –CH_3), 1.50–0.90 (m, 10H, BEt_2), 3.84 (m, 4H, $H^{3,4}$), 3.98 (m, 4H, $H^{2,5}$).

4.4. Crystal structure determination of the spirotin compound 5b

A single crystal of **5b**, recrystallised from hexane at −20 °C, was sealed under argon in a Lindemann capillary. Intensity data collection was carried out on a Siemens P4 diffractometer with Mo–K_α-radiation ($\lambda = 71.073$ pm, graphite monochromator) at r.t. The hydrogens are in calculated positions. All non-hydrogen atoms were refined with anisotropic temperature factors. The hydrogen atoms were refined applying the riding model with fixed isotropic temperature factors.

5b: $C_{32}H_{59}BFeN_2Si_4Sn$, yellow prism of dimensions $0.18 \times 0.14 \times 0.10$ mm, crystallizes monoclinically, space group $P2_1/n$; $a = 1126.3(3)$, $b = 1617.6(4)$, $c = 2280.3(6)$ pm, $\beta = 104.077(9)^\circ$, $Z = 4$, $\mu = 1.121$ mm^{-1}; 4835 reflections collected in the range 2–20° in ϑ, 3665 reflections independent, 3142 reflections assigned as observed ($I > 2\sigma(I)$); the structure was solved and refined using the program package SHELTX V.5.1; full-matrix least-squares refinement with 370 parameters, R_1/wR_2-values 0.0314/0.0902, no absorption correction (an attempted absorption correction did not improve the significance of the structural parameters); max./min. residual electron density 0.533/−0.814 e × 10^{-6} pm^{-3}.

5. Supplementary information

Crystallographic data (excluding structure factors) for the structure reported in this paper have been deposited with the Cambridge Crystallographic Data Centre CCDC no. 203953 for compound **5b**. Copies of this information may be obtained free of charge from The Director, CCDC, 12 Union Road, Cambridge CB2 1EZ, UK (Fax (internat): +44-1223-336-033; e-mail deposit@ccdc.cam.ac.uk or www: http://www.ccdc.cam.ac.uk).

Acknowledgements

This work was supported by the Deutsche Forschungsgemeinschaft and the Fonds der Chemischen Industrie. We thank the companies Bruker and Varian for running some of the liquid and solid-state NMR experiments.

References

[1] B. Wrackmeyer, Coord. Chem. Rev. 145 (1995) 125.
[2] (a) J. Dubac, A. Laporterie, G. Manuel, Chem. Rev. 90 (1990) 215;
(b) F.C. Leavitt, T.A. Manuell, F. Johnson, L.K. Matternas, D.S. Lehman, J. Am. Chem. Soc. 82 (1960) 5099;
(c) A.J. Ashe, III, D.R. Diephouse, J. Organomet. Chem. Sect. C 202 (1980) 95;
(d) P.J. Fagan, W.A. Nugent, J. Am. Chem. Soc. 110 (1988) 2310;
(e) P.J. Fagan, W.A. Nugent, J.C. Calabrese, J. Am. Chem. Soc. 116 (1994) 1880;
(f) J. Krause, K.-J. Haack, K.-R. Poerschke, B. Gabor, R. Goddard, C. Pluta, K. Seevogel, J. Am. Chem. Soc. 118 (1996) 804.
[3] B. Wrackmeyer, A. Pedall, W. Milius, O.L. Tok, Yu.N. Bubnov, J. Organomet. Chem. 649 (2002) 232.
[4] B. Wrackmeyer, W. Milius, H.E. Maisel, H. Vollrath, M. Herberhold, Z. Anorg. Allg. Chem. (2003) in press.
[5] (a) A. Shafir, M.P. Power, G.D. Whitener, J. Arnold, Organometallics 19 (2000) 2987;
(b) A. Shafir, M.P. Power, G.D. Whitener, J. Arnold, Organometallics 20 (2001) 1365;
(c) A. Shafir, J. Arnold, J. Am. Chem. Soc. 123 (2001) 9212.
[6] (a) B. Wrackmeyer, K. Horchler, R. Boese, Angew. Chem. 101 (1989) 1563; Angew. Chem. Int. Ed. Engl. 28 (1989) 1500.;
(b) B. Wrackmeyer, G. Kehr, R. Boese, Angew. Chem. 103 (1991) 1374; Angew. Chem. Int. Ed. Engl. 30 (1991) 1370.;
(c) B. Wrackmeyer, S. Kundler, R. Boese, Chem. Ber. 126 (1993) 1361;
(d) B. Wrackmeyer, G. Kehr, S. Ali, Inorg. Chim. Acta 216 (1994) 51.
[7] (a) B. Wrackmeyer, G. Kehr, R. Boese, Chem. Ber. 125 (1992) 643;

(b) B. Wrackmeyer, U. Klaus, W. Milius, E. Klaus, T. Schaller, J. Organomet. Chem. 517 (1996) 235.
[8] B. Wrackmeyer, J. Organomet. Chem. 364 (1989) 331.
[9] R. Boese, D. Bläser, N. Niederprüm, M. Nüsse, W.A. Prett, P. von R. Schleyer, M. Bühl, N.J.R. van Eikema Hommes, Angew. Chem. 104 (1992) 356; Angew. Chem. Int. Ed. Engl. 21 (1992) 31.
[10] H. Nöth, B. Wrackmeyer, in: P. Diehl, E. Fluck, R. Kosfeld (Eds.), Nuclear Magnetic Resonance Spectroscopy of Boron Compounds NMR—Basic Principles and Progress, vol. 14, Springer, Berlin, 1978.
[11] (a) J. Stonehouse, P. Adell, J. Keeler, A.J. Shaka, J. Am. Chem. Soc. 116 (1994) 6037;
(b) K. Stott, J. Stonehouse, J. Keeler, T.-L. Hwang, A.J. Shaka, J. Am. Chem. Soc. 117 (1995) 4199.
[12] (a) G.A. Morris, R. Freeman, J. Am. Chem. Soc. 101 (1979) 760;
(b) G.A. Morris, J. Am. Chem. Soc. 102 (1980) 428;
(c) G.A. Morris, J. Magn. Reson. 41 (1980) 185;
(d) D.P. Burum, R.R. Ernst, J. Magn. Reson. 39 (1980) 163.
[13] A. Bax, R. Freeman, J. Am. Chem. Soc. 108 (1986) 2093.
[14] W. Wilker, D. Leibfritz, R. Kersebaum, W. Bermel, Magn. Reson. Chem. 31 (1993) 287.
[15] B. Wrackmeyer, Progr. NMR Spectrosc. 12 (1979) 227.
[16] (a) A.C. Olivieri, J. Magn. Reson. 81 (1989) 201;
(b) R.K. Harris, P. Jonson, K.J. Packer, C.D. Campbell, Magn. Reson. Chem. 24 (1986) 977;
(c) S. Wi, L. Frydman, J. Phys. Chem. 112 (2000) 3248.
[17] (a) H. Barjat, D.L. Mattiello, R. Freeman, J. Magn. Reson. 136 (1999) 114;
(b) X.-A. Mao, C.-H. Ye, Concepts Magn. Reson. 9 (1997) 173.
[18] B. Wrackmeyer, G. Kehr, H. Zhou, S. Ali, Main Group Met. Chem. 15 (1992) 89.
[19] (a) B. Wrackmeyer, Annu. Rep. NMR Spectrosc. 16 (1985) 73;
(b) B. Wrackmeyer, Annu. Rep. NMR Spectrosc. 38 (1999) 203.
[20] J.C. Martins, M. Biesemanns, R. Willem, Prog. NMR Spectrosc. 36 (2000) 271.
[21] (a) A. Sebald, in: M. Gielen, R. Willem, B. Wrackmeyer (Eds.), Advanced Applications of NMR to Organometallic Chemistry, Physical Organometallic Chemistry, vol. 1, Wiley, Chichester, 1996, pp. 123–157;
(b) A. Sebald, in: P. Diehl, E. Fluck, H. Günther, R. Kosfeld, J. Seelig (Eds.), Solid-State NMR II, NMR Basic Principles and Progress, vol. 31, Springer, Berlin, 1994, pp. 91–131.
[22] O.B. Peersen, X. Wu, S.O. Smith, J. Magn. Reson. A 106 (1994) 127.